Acta Crystallographica Section B
Structural Science
ISSN 0108-7681

Hexagonal Frank–Kasper phases interpreted as modulated crystals

Masaya Uchida* and Yoshio Matsui

Advanced Materials Laboratory, National Institute for Materials Science, Tsukuba, Ibaraki, 305-0044, Japan

Correspondence e-mail: uchida.masaya@nims.go.jp

Received 13 January 2001
Accepted 11 April 2001

The structures of the hexagonal Frank–Kasper phases F and K, which have been described in terms of the aggregation of clusters, are interpreted as modulated crystal structures. They are basically composed of two close-packed layers with ordered atomic vacancies rotated by 90° to each other about their normal.

1. Introduction

Frank & Kasper (1958, 1959) discussed the analysis and classification of complex alloys on the basis of sphere packing using the concept of triangulated coordination shells. Frank–Kasper (FK) phases are classified as having tetrahedrally close-packed (t.c.p.) structures containing interpenetrating polyhedra with coordination numbers 12, 14, 15 or 16 (Frank & Kasper, 1958, 1959; Shoemaker & Shoemaker, 1969; Nelson & Spaepen, 1989). Frank & Kasper (1958, 1959) also showed that most of these t.c.p. structures are layer structures consisting of juxtaposed hexagonal and/or pentagonal antiprisms. Shoemaker & Shoemaker (1969) classified these t.c.p. structures according to the main polygons in the primary layer, giving three categories: hexagons, pentagons and a mixture of the two. Anderson (1978) pointed out that some complex t.c.p. structures can be derived from a simple structure type, the β-tungsten structure by crystallographic operations such as translation, rotation, reflection and intergrowth. In these analyses the structure is analyzed in terms of short-range ordering of elemental structures such as clusters (or polyhedra, tiling, antiprisms, polygons *etc.*).

Hexagonal FK phases are classified as t.c.p. structures consisting mainly of hexagonal antiprisms. The simplest cases are the cubic Cr_3Si and hexagonal Zr_4Al_3 structures. Frank & Kasper (1958, 1959) took up the tilings composed of squares and equilateral triangles and showed that the atoms in Cr_3Si form deformed hexagonal antiprisms arranged in a square pattern and those in Zr_4Al_3 are arranged in a hexagonal pattern. Wang *et al.* (1989) used the projection method to describe the structures of the hexagonal FK phases such as the K phase.

Recently, we presented a new interpretation of complex alloys related to an icosahedron (coordination number 12), such as the μ-Al_4Mn phase as modulated crystals (Uchida & Horiuchi, 1999; Uchida & Matsui, 2000; Uchida & Matsui, 2001). It was shown that the structure is basically composed of close-packed layers with ordered atomic vacancies due to the occurrence of charge-density waves. This interpretation is essentially different from the idea of packing clusters in the following respect: the existence of a basic structure with long-range translational periodicity such as a close-packed layer. In

the present paper we report a similar study to see whether our interpretation without clusters can be extended to the hexagonal FK phases, which have been described in terms of the aggregation of clusters. Examples are the F (Li & Kuo, 1986; Lin & Steeds, 1986) and K (Li & Kuo, 1986) phases in a Ni-based super alloy. That is to say we interpret these phases from the viewpoint of the modulated crystal. It is shown that intense diffraction spots come from close-packed layers with long-range translational periodicity and weak ones are due to an arrangement of atomic vacancies.

2. Two examples of the hexagonal FK phases

2.1. F phase

The F phase is one of the hexagonal FK phases and exists in the region with a composition close to $Cr_{41}Co_{20}Ni_{12}Mo_{16}W_{11}$ (Lin & Steeds, 1986) or $Mo_{45}W_{11}Ni20Cr_{24}$ (Li & Kuo, 1986). Lin & Steeds (1986) and Li & Kuo (1986) independently determined the structure of the F phase with a hexagonal unit cell ($P6/mmm$, $a = b = 12.6$, $c = 4.6$ Å) by electron microscopy and described it in terms of the aggregation of clusters. Fig. 1(*a*) shows the projection of the structure along the [001] axis. The atomic parameters determined by Lin & Steeds (1986) were used. The structure is composed of four layers stacked perpendicularly to the [001] axis, *i.e.* two primary layers and two secondary layers. The two primary layers at $z = 0$ and $\frac{1}{2}$ are formed by tessellations of triangles and hexagons. Atoms of the two identical secondary layers at $z = 1/4$ and 3/4 are located at the center of the hexagonal antiprisms formed by the superposition of the primary layers.

Here, we interpret the F phase from the viewpoint of the modulated crystal. We now focus on the primary layers at $z = 0$ and $\frac{1}{2}$. Solid circles in Fig. 1(*b*) represent atoms in the primary layer at $z = 0$, gray circles in Fig. 1(*c*) those in the primary layer at $z = \frac{1}{2}$. The center of the hexagon in the primary layer, marked by squares, is unoccupied. Here we refer to this as the atomic vacancy site in the close-packed layer. It is then understood that the two primary layers are two close-packed layers with ordered atomic vacancies rotated by 90° to each other about their normal. Atoms in the secondary layers are located above and below the atomic vacancy sites in the primary layers.

To elucidate the features of the primary layer in reciprocal space, we calculated the intensity distribution in electron diffraction patterns (EDPs) from the primary layers at $z = 0$ and $\frac{1}{2}$. The result is shown in Figs. 2(*a*) and (*b*). The spot positions can be interpreted by a modulated crystal as follows. In the case of the primary layer at $z = 0$, intense spots located at the intersections of solid lines are the basic spots. The reciprocal lattice unit vectors $\mathbf{g}_{100}$ and $\mathbf{g}_{010}$ corresponding to the basic spots have a magnitude of 0.48 Å^{-1} and the indices in the figure are based on the basic hexagonal lattice. It should be noted that there is a periodic repetition of the positions of the diffraction spots *via* the translation of the reciprocal lattice vector of the basic hexagonal lattice. The other weak spots can be explained by assuming modulation waves. First-order modulation wavevectors cannot be uniquely identified because the structure refinement has not been performed. For example, we can choose three modulation waves as follows. The three modulation waves have commensurate modulation vectors $\mathbf{q}_i$ ($i = 1, 2, 3$) with a magnitude of $(4/9)|\mathbf{g}_{110}|$ along the three equivalent $\mathbf{g}_{110}$ directions, where $\mathbf{g}_{110}$ is the wavevector for the 110 basic spot. Among these three wavevectors, only two are linearly independent. A diffraction vector $\mathbf{H}$ can be written as

$$\mathbf{H} = h\mathbf{g}_{100} + k\mathbf{g}_{010} + \sum_{i=1}^{3} m_i\mathbf{q}_i,$$

where h, k and the m_i are integers. For example, spots indicated with marks A and B in Fig. 2(*a*) correspond to the higher-order satellite spots of $2\mathbf{q}_1 - \mathbf{q}_2 - 2\mathbf{g}_{100} - \mathbf{g}_{010}$ and $-3\mathbf{q}_1$

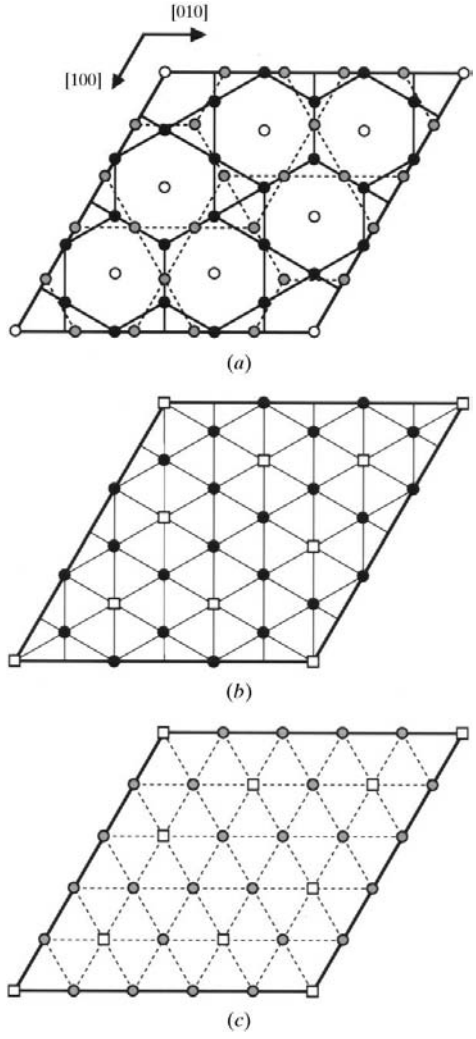

Figure 1
(*a*) Projection of the F phase along the [001] axis. The solid circles represent atoms in the primary layer at $z = 0$ and gray circles at $z = \frac{1}{2}$, forming hexagonal antiprisms. The open circles represent atoms in the secondary layers at $z = \frac{1}{4}$ and $\frac{3}{4}$, which are located at the center of the hexagonal antiprisms. (*b*) Structure in the primary layer at $z = 0$. The solid circles represent atoms. The squares represent the atomic vacancy sites. A triangular net represents a close-packed layer. (*c*) Structure in the primary layer at $z = \frac{1}{2}$. The gray circles represent atoms.

$-3\mathbf{q}_2 + 2\mathbf{g}_{010}$, respectively. In the case of the primary layer at $z = 1/2$, intense spots located at the intersections of dashed lines are the basic spots. The reciprocal lattice unit vectors $\mathbf{G}_{100}$ and $\mathbf{G}_{010}$ corresponding to the basic spots have a magnitude of 0.46 Å^{-1} and the indices in the figure are based on the basic hexagonal lattice. The hexagonal net generated by wavevectors $\mathbf{G}_{100}$ and $\mathbf{G}_{010}$ has a relative orientation of 90° to that by wavevectors $\mathbf{g}_{100}$ and $\mathbf{g}_{010}$. The other weak spots can be explained by assuming three modulation waves. The three modulation waves have commensurate modulation vectors $\mathbf{Q}_i$ (i = 1, 2, 3) with a magnitude of $(2/5)|\mathbf{G}_{110}|$ along the three equivalent $\mathbf{G}_{110}$ directions, where $\mathbf{G}_{110}$ is the wavevector for the 110 basic spot. For example, spots indicated with marks C and D in Fig. 2(b) correspond to the higher-order satellite spots of $-2\mathbf{Q}_1 - \mathbf{Q}_2 + \mathbf{G}_{010}$ and $2\mathbf{Q}_1 + 3\mathbf{Q}_2 + \mathbf{G}_{100} - \mathbf{G}_{010}$, respectively. The calculated EDP of the F phase (Fig. 2c) can be essentially obtained by superposing two sets of patterns from two primary layers. This implies that the proper use of a 'hidden symmetry' such as a close-packed layer, which does not appear in space-group symmetry, would be helpful in the structure solution of phases related to the hexagonal FK phases. Actually, we used the 'hidden symmetry' to create the structure model for the 12-fold quasicrystal (Uchida & Horiuchi, 1998).

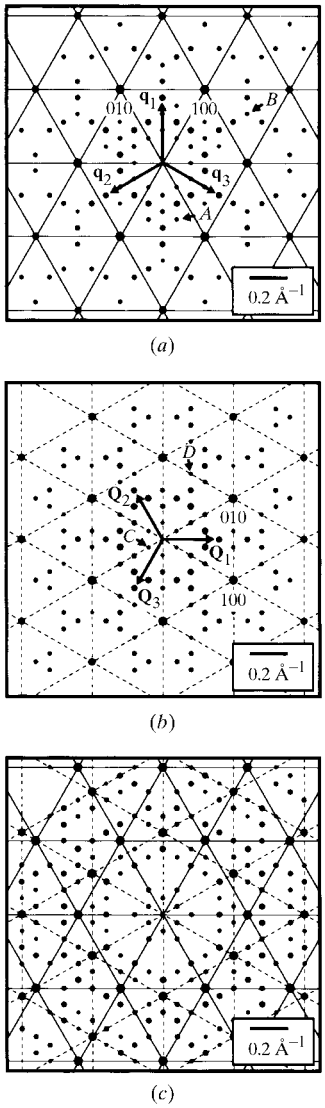

Figure 2
Calculated EDPs from the primary layer (a) at $z = 0$, (b) at $z = \frac{1}{2}$ and (c) from the F phase along ⟨001⟩ based on the assumption that all the atoms are Cr atoms. The diffraction spots located at the intersections of the solid and dashed lines are the basic spots. The radius of the diffraction spots is proportional to the diffraction intensity. The indices are based on the basic hexagonal lattice. The EDP of the F phase (Fig. 2c) can be essentially obtained by superposing two sets of patterns (Figs. 2a and b) from two primary layers.

2.2. K phase

The K phase is one of the hexagonal FK phases and coexists with the F phase (Li & Kuo, 1986). Li & Kuo (1986) deter-

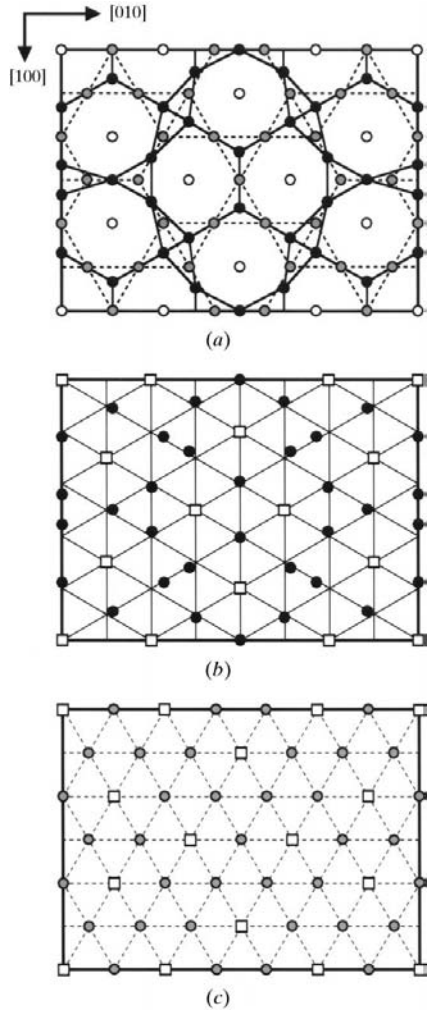

Figure 3
(a) Projection of the K phase along the [001] axis. The solid circles represent atoms in the primary layer at $z = 0$ and gray circles at $z = \frac{1}{2}$, forming hexagonal antiprisms. The open circles represent atoms in the secondary layers at $z = \frac{1}{4}$ and $\frac{3}{4}$, which are located at the center of the hexagonal antiprismes. (b) Structure in the primary layer at $z = 0$. The solid circles represent atoms. The squares represent the atomic vacancy sites. A triangular net represents a slightly distorted close-packed layer. (c) Structure in the primary layer at $z = \frac{1}{2}$. The gray circles represent atoms.

mined the structure of the K phase with an orthorhombic unit cell (*Pmmm*, a = 12.5, b = 17.1, c = 4.5 Å) by electron microscopy and described it in terms of the aggregation of clusters. Fig. 3(*a*) shows the projection of the structure along the [001] axis. The structure is made of four layers stacked perpendicularly to the [001] axis, *i.e.* two primary layers and two secondary layers. The two primary layers at z = 0 and $\frac{1}{2}$ are formed by tessellations of triangles and hexagons. Atoms of the two identical secondary layers at z = 1/4 and 3/4 are located at the center of the hexagonal antiprisms formed by the superposition of the primary layers.

We now focus on the primary layers at z = 0 and 1/2. Solid circles in Fig. 3(*b*) represent atoms in the primary layer at z = 0, gray circles in Fig. 3(*c*) those in the primary layer at $z = \frac{1}{2}$. Although some atoms in the primary layer at z = 0 displace largely, it is understood that the two primary layers are two slightly distorted close-packed layers with ordered atomic vacancies rotated by 90° to each other about their normal as in the F phase.

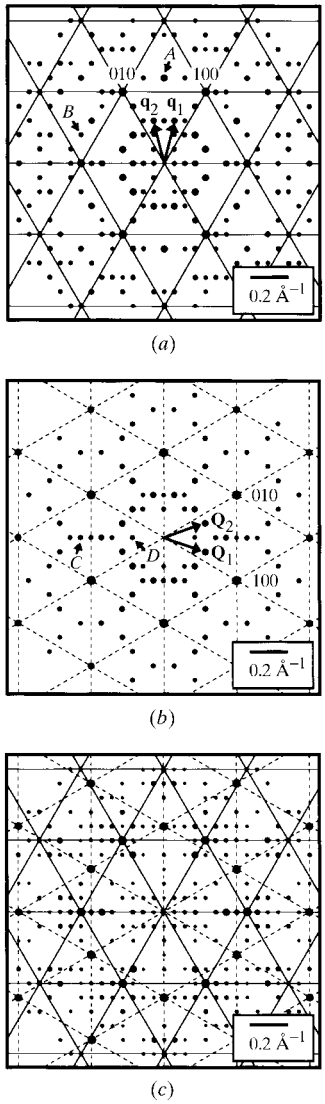

Figure 4
Calculated EDPs from the primary layer (*a*) at z = 0, (*b*) at $z = \frac{1}{2}$ and (*c*) from the K phase along ⟨001⟩ based on the assumption that all the atoms are Mo atoms. The diffraction spots located at the intersections of the solid and dashed lines are the basic spots. The radius of the diffraction spots is proportional to the diffraction intensity. The indices are based on the basic pseudo-hexagonal lattice. The EDP of the F phase (Fig. 4*c*) can be essentially obtained by superposing two sets of patterns (Fig. 4*a* and *b*) from two primary layers.

To elucidate the features of the primary layer in reciprocal space, we calculated the intensity distribution in EDPs from the primary layers at z = 0 and $\frac{1}{2}$. The result is shown in Figs. 4(*a*) and (*b*). In the case of the primary layer at z = 0, intense spots located at the intersections of solid lines are the basic spots. The reciprocal lattice unit vectors $\mathbf{g}_{100}$ and $\mathbf{g}_{010}$ corresponding to the basic spots have a magnitude of 0.46 Å^{-1} and create an angle of 60.6° to each other. The indices in the figure are based on the basic pseudo-hexagonal lattice. The other weak spots can be explained by assuming modulation waves. First-order modulation wavevectors cannot be uniquely identified because the structure refinement has not been performed. For example, we can choose two commensurate modulation waves as follows. The modulation vectors $\mathbf{q}_i$ (i = 1, 2) are $(17/40)\mathbf{g}_{100} + (7/40)\mathbf{g}_{010}$ and $(7/40)\mathbf{g}_{100} + (17/40)\mathbf{g}_{010}$, respectively. A diffraction vector $\mathbf{H}$ can be written as

$$\mathbf{H} = h\mathbf{g}_{100} + k\mathbf{g}_{010} + \sum_{i=1}^{2} m_i\mathbf{q}_i,$$

where h, k and m_i are integers. For example, spots indicated with marks A and B in Fig. 4(*a*) correspond to the higher-order satellite spots of $\mathbf{q}_1 + \mathbf{q}_2$ and $2\mathbf{q}_1 + 2\mathbf{q}_2 - 2\mathbf{g}_{100}$, respectively. In the case of the primary layer at $z = \frac{1}{2}$, the reciprocal lattice unit vectors $\mathbf{G}_{100}$ and $\mathbf{G}_{010}$ corresponding to the basic spots have a magnitude of 0.47 Å^{-1} and create an angle of 60.8° to each other. The indices in the figure are based on the basic pseudo-hexagonal lattice. The other weak spots can be explained by assuming commensurate modulation waves. The two modulation vectors $\mathbf{Q}_i$ (i = 1, 2) are $(19/42)\mathbf{G}_{100} + (5/42)\mathbf{G}_{010}$ and $(5/42)\mathbf{G}_{100} + (19/42)\mathbf{G}_{010}$, respectively. For example, spots indicated with marks C and D in Fig. 4(*b*) correspond to the higher-order satellite spots of $-\mathbf{Q}_1 - \mathbf{Q}_2$ and $-\mathbf{Q}_1 + 2\mathbf{Q}_2 - \mathbf{G}_{010}$, respectively. The calculated EDP of the K phase (Fig. 4*c*) can be essentially obtained by superposing two sets of patterns from two primary layers.

3. Conclusions

We have given two examples. According to this new interpretation, the other hexagonal FK phases (Nelson & Spaepen, 1989) such as the σ phase and the J phase can be understood to be modulated crystals (Uchida, 2000). This approach will be helpful in the study of the hexagonal FK phases.

The authors would like to thank Drs S. Horiuchi and A. Yamamoto of NIMS for discussions.

References

Anderson, S. (1978). *J. Solid State Chem.* **23**, 191–204.
Frank, F. C. & Kasper, J. S. (1958). *Acta Cryst.* **11**, 184–190.

Frank, F. C. & Kasper, J. S. (1959). *Acta Cryst.* **12**, 483–499.
Li, D. X. & Kuo, K. H. (1986). *Acta Cryst.* B**42**, 152–159.
Lin, Y. P. & Steeds, J. W. (1986). *Acta Cryst.* B**42**, 159–162.
Nelson, D. R. & Spaepen, F. (1989). *Solid State Physics*, edited by H. Ehrenreich and D. Turnbull, pp. 1–90. Boston: Academic Press.
Shoemaker, C. B. & Shoemaker, D. P. (1969). *Developments in the Structural Chemistry of Alloy Phases*, pp. 107–139. New York: Plenum Press.
Uchida, M. (2000). Unpublished work.
Uchida, M. & Horiuchi, S. (1998). *J. Appl. Cryst.* **31**, 634–637.
Uchida, M. & Horiuchi, S. (1999). *J. Appl. Cryst.* **32**, 417–420.
Uchida, M. & Matsui, Y. (2000). *Acta Cryst.* B**56**, 654–658.
Uchida, M. & Matsui, Y. (2001). *Philos. Mag. A.* In the press.
Wang, Z. M., Yang, Q. B. & Kuo, K. H (1989). *Acta Cryst.* A**45**, 268–274.